Dynamic Analysis of Carbon Nanotube-Reinforced Multilayer Composite Plates

Jamshid Ebrahimi, Jafar Eskandari Jam *, Reza Azarafza, Mohsen Heydari Beni
Department of Mechanical Engineering,
Malek Ashtar University of Technology, Tehran, Iran
E-mail: jejam@mail.com, eskandari@mut.ac.ir, azarmut@mut.ac.ir, mohsenheydari1371@gmail.com
*Corresponding author

Majid Eskandari Shahraki
Department of Aerospace Engineering,
Ferdowsi University of Mashhad, Iran
E-mail: mjdeskandari@gmail.com

Received: 22 July 2020, Revised: 13 August 2020, Accepted: 2 September 2020

Abstract: The paper studied the analysis of vibrations of rectangular carbon nanotube-reinforced composite plates. To this end, a three-layer nanocomposite plate - two layers with the targeted distribution of carbon nanotubes as FG-X at the top and bottom and a layer without an amplifier in the middle of the plate - were analyzed. The governing equations for this problem are based on First-order Shear Deformation Theory (FSDT). The distribution of nanotubes on these plates is as targeted FG-X. The effect of various types of SWCNTs distributions in the direction of thickness on the vibrational behavior of nanocomposite plates was examined. The effective properties of nanocomposite materials Functionally Graded Carbon Nanotube-Reinforced Composite (FG-CNTRC) were estimated using the rule of mixtures. Detailed parametric studies were performed to determine the effects of the volume fraction of carbon nanotubes and the thickness-to-length ratio of the plate on the natural frequency responses and the shape of the plate mode. The equations obtained in this problem were coded in MATLAB software, the nanocomposite plate was modelled in ABAQUS software, and the comparison of the results obtained from the numerical solution with ABAQUS software showed relatively right consistency with the results obtained from the analytical solution.

Keywords: Composite Plates, Carbon Nanotubes, Finite Element, FSDT, Vibrations

Reference: Jamshid Ebrahimi, Jafar Eskandari Jam, Reza Azarafza, Mohsen Heydari Beni, and Majid Eskandari Shahraki, "Dynamic Analysis of Carbon Nanotube-Reinforced Multilayer Composite Plates", Int J of Advanced Design and Manufacturing Technology, Vol. 14/No. 1, 2021, pp. 115–128.
DOI: 10.30495/admt.2021.1905074.1206

Biographical notes: Jamshid Ebrahimi received his MSc, in Mechanical Engineering from University of Malek Ashtar. His field of research is mechanical analysis of composite materaials. **Jafar Eskandari Jam** is Professor of Mechanical engineering at Malek Ashtar University Tehran, Iran. His current research focuses on composite structures, plates and shell analysis and nanomechanics. **Rreza Azarafza** is currently Assistant Professor at the Department of Mechanical Engineering, at Malek ashtar University, Tehran, Iran. His current research interest includes composite manufacturing and composite structures. **Mohsen Heydari Beni**, is currently a PhD student at Malek Ashtar University and his main research interests are composite structures, plates and shell analysis and nanomechanics. **Majid Eskandari Shahraki** is currently a PhD student at Ferdowsi University of Mashhad, Iran and his main research interests is nanomechanics.

1 INTRODUCTION

Carbon Nanotubes (CNTs) were discovered by Iijima in 1991 [1]. Overall, carbon nanotubes are as Single Wall Carbon Nanotube (SWCNT), Multi-Wall Carbon Nanotube (MWCNT) or rope. Young's modulus and the strength of carbon nanotubes are much larger than those of conventional materials and metals, at about 1,000 and 50 gigapascals (GPa), respectively. Carbon nanotubes have extraordinary properties like stiffness to weight ratio and strength to weight ratio [2].

The paper has examined the effect of using SWCNTs in the vibrational analysis of a rectangular nanocomposite plate. The purpose of using carbon nanotubes is to increase damping to prevent damage caused by resonance and to enhance the mechanical properties of the structure. The nanotubes used are of single-wall type used in various weight percentages, including 0.11, 0.14 and 0.17. After analysing the problem, the values of natural frequencies and damping coefficients are obtained in different vibrational modes. Moreover, frequency analysis is performed and compared with the results of the analytical method by calculating the mechanical properties of Carbon Nanotube-Reinforced Composite (CNTRC) and modelling it in ABAQUS finite element software.

Lei et al. [3] have studied the free vibrations of CNTRC in a thermal environment. The nanotubes used in this study had used SWCNT (types 10 and 10). Four types of nanotube distributions are described in CNTRC plates with length a, width b and thickness h, identified with UD, FG-V, FG-O and FG-X indices. The governing equations in their study are based on First Order Shear Deformation Theory (FSDT). They found that the higher the volume fraction of CNTs, the higher the volume fraction of nanotubes in the range (0.11 - 0.22) and the higher the natural frequency will be. Nami et al. [4] have analysed the free vibrations of thick rectangular composite plates reinforced with targeted carbon nanotubes based on three-dimensional differential theory and using Differential Quadrature Method (DQM). Alibegloo et al. [5] analysed free vibrations and bending of CNTRC based on the three-dimensional elasticity theory by DQM. The nanotubes used are single-wall, the distribution of CNTs in the field is the Uniform Distribution (UD), and there are three types of targeted FG-V, FG-O and FG-X.

Asadi et al. [2] have experimentally examined the vibrational properties of multi-layered carbon nanotube reinforced composites. The composite in question is made of glass / epoxy to which multi-wall and single-wall carbon nanotubes have been added in various mass percentages. CNTs were first distributed in an epoxy process to prepare the samples. Amraei et al. [6] have studied the free vibrations of multilayer rectangular composite plates reinforced with carbon nanotubes. The distribution of nanotubes within the polymer is random. The methods used for analysis are based on Classical Laminated Plate Theory (CLPT), FSDT, and Third Order Shear Deformation Theory (TSDT) theory with simply supported boundary conditions (SSSS). The effective properties of nanotube-reinforced polymer materials are based on Cox model. Moreover, the calculation of the properties of multilayer materials is based on the rule of mixture and Halpin-Tsai equation. Ngo Dinh Dat et al. [7] presented an analytical solution for the non-linear magnetic vibrations of the electro-elastic smart sandwich plate with a carbon nanocomposite core reinforced with carbon nanotubes in a humid environment. In this paper, vibrations of rectangular carbon nanotube-reinforced three-layer composite plates were analysed.

2 EFFECTIVE PROPERTIES OF CNTRC LAYER MATERIALS

The type of carbon nanotubes used in this study is SWCNTs, and the material properties of carbon nanotubes are obtained based on Molecular Dynamics (MD) simulations. The effective properties of nanocomposite materials, a mixture of carbon nanotubes and isotropic polymers, can be estimated based on the Mori Tanaka (M - T) design [8] or the law of mixtures [9-10]. In this study, the rule of modified mixtures is used to obtain the effective parameters and effective properties of CNTRC used as follows [11]:

$$E_{11} = \eta_1 V_{CN} E_{11}^{CN} + V_M E^M \tag{1}$$

$$\frac{\eta_2}{E_{22}} = \frac{V_{CN}}{E_{22}^{CN}} + \frac{V_M}{E^M} \tag{2}$$

$$\frac{\eta_3}{G_{12}} = \frac{V_{CN}}{G_{12}^{CN}} + \frac{V_M}{G^M} \tag{3}$$

$$\upsilon_{12} = V_{CNT}^{*} \upsilon_{12}^{CNT} + V_m \upsilon_m \tag{4}$$

$$\rho = V_{CNT} \rho^{CNT} + V_m \rho^m \tag{5}$$

Here, E_{11}^{CN} and E_{22}^{CN} are, respectively, Young's modulus of longitudinal and transverse of carbon nanotubes, G_{12} is shear modulus of carbon nanotubes, and E^M and G^M are similar properties for the matrix and $\eta_J (J = 1,2,3)$ are quality parameters of CNTs, which are

determined by matching the elastic constants of the CNTRC plate by molecular dynamics simulation [11]. Moreover, V_{CN} and V_M are, respectively, volumetric fractions of CNTs and the matrix, satisfied by equation $V_M + V_{CN} = 1$. α_{11} and α_{22} are the coefficients of thermal expansion in the longitudinal and transverse directions of CNTRC plates, respectively, and are obtained from the following equations [12]:

$$\alpha_{11} = V_{CNT}\,\alpha_{11}^{CNT} + V_m \alpha^m \tag{6}$$

$$\alpha_{22} = (1+\upsilon_{12}^{CNT})\,V_{CNT}\,\alpha_{22}^{CNT} + (1+\upsilon^m)\,V_m \alpha^m - \upsilon_{12}\alpha_{11} \tag{7}$$

Here, α_{11}^{CNT}, α_{22}^{CNT} and α^m are, respectively, the coefficients of longitudinal and transverse thermal expansion of nanotubes and the ratio of thermal expansion of the matrix. Given the above equations and "Fig. 1", one can calculate the material properties of every single layer. As is seen in the figure below, this laminate consists of three layers.

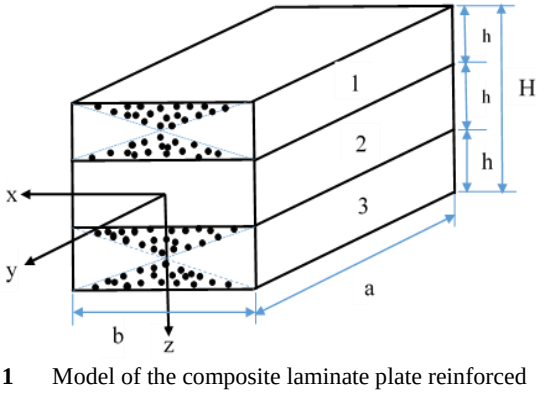

Fig. 1 Model of the composite laminate plate reinforced with carbon nanotubes.

The distribution of nanotubes in layers 1 and 3 is FG-CNTRC distributed in as FG-X, and layer 2 only has the isotropic base material of epoxy resin. Thus, one concludes that equations (1) to (5) are used to obtain the properties of materials in layers 1 and 3, and equation (8) is used to calculate the properties of materials in layer 2 [13].

$$\begin{cases} G_m = \dfrac{E_m}{2*(1+\upsilon_m)} \\ E_{11} = E_{22} = E_{33} = E_m \\ G_{12} = G_{13} = G_{23} = G_m \\ \upsilon_{12} = \upsilon_{13} = \upsilon_{23} = \upsilon_m \\ \rho = \rho_m \end{cases} \tag{8}$$

Other effective mechanical properties are:

$$\begin{cases} E_{33} = E_{22},\ G_{13} = G_{12},\ G_{23} = 1.2\ G_{12}, \\ \upsilon_{13} = \upsilon_{12},\ \upsilon_{31} = \upsilon_{21},\ \upsilon_{32} = \upsilon_{23} = \upsilon_{21}, \\ \upsilon_{21} = \dfrac{E_{22}}{E_{11}}\upsilon_{12} \end{cases} \tag{9}$$

3 DISTRIBUTION OF SINGLE-WALL NANOTUBES (SWCNTS 10,10) IN THE DIRECTION OF THICKNESS

Ordinary geometry shows a symmetrical multi-layered nanocomposite plate with targeted distribution of CNTs in layers 1 and 3 as FG-X, with length a and width b and thickness H and with xyz coordinate system, as shown in "Fig. 1". In solving this problem, it is assumed layers 1 and 3 of the matrix are reinforced by CNTs and their volume fraction depends on the following equation [12]:

$$V_M + V_{CN} = 1 \tag{10}$$

In addition, the distribution function of CNTs inside the matrix is as follows [14]:

$$V_{CNT}(z) = 2\left(2\frac{|z|}{h}\right)V_{CNT}^* \tag{11}$$

This function is used only for calculating I_0, I_1, I_2 [13].

$$V_{CNT}^* = \frac{W_{CNT}}{W_{CNT} + \left(\dfrac{\rho_{CNT}}{\rho_m}\right) - \left(\dfrac{\rho_{CNT}}{\rho_m}\right)W_{CNT}} \tag{12}$$

$$W_{CNT} = \frac{\rho_{CNT}}{\rho_{CNT} + \rho_m} \tag{13}$$

W_{CNT} is the mass fraction of carbon nanotubes on CNTRC plates, and V_{CNT}^* is the volumetric fraction of carbon nanotubes on CNTRC plates.

4 THEORETICAL FSDT OF CNTRC PLATES

FSDT has been used to analyze this problem; the displacement field in this theory is usually as follows [15]:

$$\begin{aligned} u(x,y,z,t) &= u_0(x,y,t) + z\,\phi_x(x,y,t) \\ v(x,y,z,t) &= v_0(x,y,t) + z\,\phi_y(x,y,t) \\ w(x,y,z,t) &= w_0(x,y,t) \end{aligned} \tag{14}$$

Here, w, v and u show displacement in directions x, y, and z, respectively. $u_0, v_0, w_0, \phi_x, \phi_y$ are unknown functions that need to be calculated, index "0" shows the displacement of the middle plate in z=0 and $\frac{\partial u}{\partial z} = \phi_x, \frac{\partial v}{\partial z} = \phi_y$ is the vertical perpendicular rotation around the axis -x and -y. In addition, strain and curvature equations are described as follows:

$$\begin{Bmatrix} \varepsilon_{xx} \\ \varepsilon_{yy} \\ \gamma_{xy} \end{Bmatrix} = \varepsilon_0 + z\,\kappa, \quad \begin{Bmatrix} \gamma_{yz} \\ \gamma_{xz} \end{Bmatrix} = \gamma_0 \tag{15}$$

$$\varepsilon_0 = \begin{Bmatrix} \frac{\partial u_0}{\partial x} \\ \frac{\partial v_0}{\partial y} \\ \frac{\partial u_0}{\partial y} + \frac{\partial v_0}{\partial x} \end{Bmatrix}, \kappa = \begin{Bmatrix} \frac{\partial \phi_x}{\partial x} \\ \frac{\partial \phi_y}{\partial y} \\ \frac{\partial \phi_x}{\partial y} + \frac{\partial \phi_y}{\partial x} \end{Bmatrix}, \quad \gamma_0 = \begin{Bmatrix} \phi_y = \frac{\partial w_0}{\partial y} \\ \phi_x = \frac{\partial w_0}{\partial x} \end{Bmatrix} \tag{16}$$

By placing equations (16) in equations (15), it is obtained:

$$\begin{Bmatrix} \varepsilon_{xx} \\ \varepsilon_{yy} \\ \gamma_{yz} \\ \gamma_{xz} \\ \gamma_{xy} \end{Bmatrix} = \begin{Bmatrix} \varepsilon_{xx}^{(0)} \\ \varepsilon_{yy}^{(0)} \\ \gamma_{yz}^{(0)} \\ \gamma_{xz}^{(0)} \\ \gamma_{xy}^{(0)} \end{Bmatrix} + z \begin{Bmatrix} \varepsilon_{xx}^{(1)} \\ \varepsilon_{yy}^{(1)} \\ \gamma_{yz}^{(1)} \\ \gamma_{xz}^{(1)} \\ \gamma_{xy}^{(1)} \end{Bmatrix} = \begin{Bmatrix} \frac{\partial u_0}{\partial x} + \frac{1}{2}\left(\frac{\partial w_0}{\partial x}\right)^2 \\ \frac{\partial v_0}{\partial y} + \frac{1}{2}\left(\frac{\partial w_0}{\partial y}\right)^2 \\ \frac{\partial w_0}{\partial y} + \phi_y \\ \frac{\partial w_0}{\partial x} + \phi_x \\ \frac{\partial u_0}{\partial y} + \frac{\partial v_0}{\partial x} + \frac{\partial w_0}{\partial x}\frac{\partial w_0}{\partial y} \end{Bmatrix} + z \begin{Bmatrix} \frac{\partial \phi_x}{\partial x} \\ \frac{\partial \phi_y}{\partial y} \\ 0 \\ 0 \\ \frac{\partial \phi_x}{\partial y} + \frac{\partial \phi_y}{\partial x} \end{Bmatrix} \tag{17}$$

Overall, the structure of the linear stress-strain equation is expressed as follows [16]:

$$\begin{Bmatrix} \sigma_{xx} \\ \sigma_{yy} \\ \sigma_{xy} \\ \sigma_{yz} \\ \sigma_{xz} \end{Bmatrix} = \begin{bmatrix} Q_{11} & Q_{12} & 0 & 0 & 0 \\ Q_{12} & Q_{22} & 0 & 0 & 0 \\ 0 & 0 & Q_{33} & 0 & 0 \\ 0 & 0 & 0 & Q_{44} & 0 \\ 0 & 0 & 0 & 0 & Q_{55} \end{bmatrix} \begin{Bmatrix} \varepsilon_{xx} \\ \varepsilon_{yy} \\ \gamma_{xy} \\ \gamma_{yz} \\ \gamma_{xz} \end{Bmatrix} \tag{18}$$

Where:

$$\begin{cases} Q_{11} = \frac{E_{11}}{1-\upsilon_{12}\upsilon_{21}}, \\ Q_{12} = \frac{\upsilon_{21}E_{11}}{1-\upsilon_{12}\upsilon_{21}}, \\ Q_{22} = \frac{E_{22}}{1-\upsilon_{12}\upsilon_{21}} \end{cases} \tag{19a}$$

$$\begin{cases} Q_{33} = G_{12}, \\ Q_{44} = G_{23}, \\ Q_{55} = G_{13}, \end{cases} \quad \begin{cases} G_{23} = 1.2G_{12} \\ \upsilon_{21} = \frac{E_{22}}{E_{11}}\upsilon_{12}, \\ G_{13} = G_{12} \end{cases}$$

$$\begin{cases} Q_{11} = Q_{22} = \frac{E_m}{1-\upsilon_m^2}, \\ Q_{12} = \frac{\upsilon_m E_m}{1-\upsilon_m^2}, \\ Q_{66} = Q_{55} = Q_{44} = G_m, \\ G_m = \frac{E_m}{2(1+\upsilon_m)} \end{cases} \tag{19b}$$

The above equations are isotropic for the middle layer (layer 2) [15]. As the plate is isotropic in terms of the arrangement of the layers, and the angle to strengthen the plates is zero, then.

$$\left[\overline{Q}\right]_{0^o} = [Q]_{0^o}$$

The results of stress-strain and curvature equations lead to the equations of force and torque [6]:

$$\begin{bmatrix} N_x \\ N_y \\ N_{xy} \end{bmatrix} = \int_{-H/2}^{H/2} \begin{bmatrix} \sigma_x \\ \sigma_y \\ \sigma_{xy} \end{bmatrix} dz, \quad \begin{bmatrix} M_x \\ M_y \\ M_{xy} \end{bmatrix} = \int_{-H/2}^{H/2} \begin{bmatrix} \sigma_x \\ \sigma_y \\ \sigma_{xy} \end{bmatrix} z dz \tag{20}$$

$$\begin{bmatrix} N_x \\ N_y \\ N_{xy} \\ M_x \\ M_y \\ M_{xy} \end{bmatrix} = \begin{bmatrix} A_{11} & A_{12} & A_{16} & B_{11} & B_{12} & B_{16} \\ A_{21} & A_{22} & A_{26} & B_{21} & B_{22} & B_{26} \\ A_{61} & A_{62} & A_{66} & B_{61} & B_{62} & B_{66} \\ B_{11} & B_{12} & B_{16} & D_{11} & D_{12} & D_{16} \\ B_{21} & B_{22} & B_{26} & D_{21} & D_{22} & D_{26} \\ B_{61} & B_{62} & B_{66} & D_{61} & D_{62} & D_{66} \end{bmatrix} \begin{bmatrix} \varepsilon_x^0 \\ \varepsilon_y^0 \\ \gamma_{xy}^0 \\ k_x \\ k_y \\ k_{xy} \end{bmatrix} \tag{21}$$

The stiffness coefficients are calculated as follows [15]:

$$A_{ij} = \sum_{k=1}^{N} Q_{ij}^{(k)} \left(z_k - z_{k-1}\right), \quad B_{ij} = \frac{1}{2}\sum_{k=1}^{N} Q_{ij}^{(k)} \left(z_k^2 - z_{k-1}^2\right), \quad D_{ij} = \frac{1}{3}\sum_{k=1}^{N} Q_{ij}^{(k)} \left(z_k^3 - z_{k-1}^3\right), \tag{22}$$

The strain and curvature of the mid-plane are given as follows [6]:

$$\varepsilon_x^0 = \frac{\partial u_0}{\partial x}, \varepsilon_y^0 = \frac{\partial v_0}{\partial y}, \gamma_{xy}^0 = \frac{\partial v_0}{\partial x} + \frac{\partial u_0}{\partial y}$$
$$k_x = -\frac{\partial^2 w_0}{\partial x^2}, k_y = -\frac{\partial^2 w_0}{\partial y^2}, k_{xy} = -2\frac{\partial^2 w_0}{\partial x \partial y} \tag{23}$$

5 EQUATIONS OF MOTION

The governing equations have been derived from FSDT using the dynamic model of the principle of virtual displacement [15]:

$$\begin{aligned} \delta u_0 &: \frac{\partial N_{xx}}{\partial x} + \frac{\partial N_{xy}}{\partial y} = I_0 \frac{\partial^2 u_0}{\partial t^2} + I_1 \frac{\partial^2 \phi_x}{\partial t^2} \\ \delta v_0 &: \frac{\partial N_{xy}}{\partial x} + \frac{\partial N_{yy}}{\partial y} = I_0 \frac{\partial^2 v_0}{\partial t^2} + I_1 \frac{\partial^2 \phi_y}{\partial t^2} \\ \delta w_0 &: \frac{\partial Q_x}{\partial x} + \frac{\partial Q_y}{\partial y} = I_0 \frac{\partial^2 w_0}{\partial t^2} \\ \delta \phi_x &: \frac{\partial M_{xx}}{\partial x} + \frac{\partial M_{xy}}{\partial y} - Q_x = I_2 \frac{\partial^2 \phi_x}{\partial t^2} + I_1 \frac{\partial^2 u_0}{\partial t^2} \\ \delta \phi_y &: \frac{\partial M_{xy}}{\partial x} + \frac{\partial M_{yy}}{\partial y} - Q_y = I_2 \frac{\partial^2 \phi_y}{\partial t^2} + I_1 \frac{\partial^2 v_0}{\partial t^2} \end{aligned} \tag{24}$$

The motion equations in FSDT can be expressed in terms of displacement terms [15]:

$$\begin{aligned} &(1): \frac{\partial N_{xx}}{\partial x} + \frac{\partial N_{xy}}{\partial y} = I_0 \frac{\partial^2 u_0}{\partial t^2} + I_1 \frac{\partial^2 \phi_x}{\partial t^2} \Rightarrow \\ &\frac{\partial}{\partial x}\left[A_{11}\frac{\partial u_0}{\partial x} + A_{12}\frac{\partial v_0}{\partial y} + A_{16}\left(\frac{\partial u_0}{\partial y} + \frac{\partial v_0}{\partial x}\right) + B_{11}\frac{\partial \phi_x}{\partial x} + B_{12}\frac{\partial \phi_y}{\partial y} + B_{16}\left(\frac{\partial \phi_x}{\partial y} + \frac{\partial \phi_y}{\partial x}\right)\right] \\ &+ \frac{\partial}{\partial y}\left[A_{16}\frac{\partial u_0}{\partial x} + A_{26}\frac{\partial v_0}{\partial y} + A_{66}\left(\frac{\partial u_0}{\partial y} + \frac{\partial v_0}{\partial x}\right) + B_{16}\frac{\partial \phi_x}{\partial x} + B_{26}\frac{\partial \phi_y}{\partial y} + B_{66}\left(\frac{\partial \phi_x}{\partial y} + \frac{\partial \phi_y}{\partial x}\right)\right] \\ &- \left(\frac{\partial N_{xx}^T}{\partial x} + \frac{\partial N_{xy}^T}{\partial y}\right) = I_0 \frac{\partial^2 u_0}{\partial t^2} + I_1 \frac{\partial^2 \phi_x}{\partial t^2} \end{aligned} \tag{25}$$

$$(2): \frac{\partial N_{xy}}{\partial x} + \frac{\partial N_{yy}}{\partial y} = I_0 \frac{\partial^2 v_0}{\partial t^2} + I_1 \frac{\partial^2 \phi_y}{\partial t^2} \Rightarrow \tag{26}$$

$$\frac{\partial}{\partial x}\left[A_{16}\frac{\partial u_0}{\partial x}+A_{26}\frac{\partial v_0}{\partial y}+A_{66}\left(\frac{\partial u_0}{\partial y}+\frac{\partial v_0}{\partial x}\right)+B_{16}\frac{\partial \phi_x}{\partial x}+B_{26}\frac{\partial \phi_y}{\partial y}+B_{66}\left(\frac{\partial \phi_x}{\partial y}+\frac{\partial \phi_y}{\partial x}\right)\right]$$
$$+\frac{\partial}{\partial y}\left[A_{12}\frac{\partial u_0}{\partial x}+A_{22}\frac{\partial v_0}{\partial y}+A_{26}\left(\frac{\partial u_0}{\partial y}+\frac{\partial v_0}{\partial x}\right)+B_{12}\frac{\partial \phi_x}{\partial x}+B_{22}\frac{\partial \phi_y}{\partial y}+B_{26}\left(\frac{\partial \phi_x}{\partial y}+\frac{\partial \phi_y}{\partial x}\right)\right]$$
$$-\left(\frac{\partial N^T_{xy}}{\partial x}+\frac{\partial N^T_{yy}}{\partial y}\right)=I_0\frac{\partial^2 v_0}{\partial t^2}+I_1\frac{\partial^2 \phi_y}{\partial t^2}$$

(3): $\frac{\partial Q_x}{\partial x}+\frac{\partial Q_y}{\partial y}=I_0\frac{\partial^2 w_0}{\partial t^2}\Rightarrow$

$$\frac{\partial}{\partial x}\left[KA_{45}\left(\frac{\partial w_0}{\partial y}+\phi y\right)+KA_{55}\left(\frac{\partial w_0}{\partial x}+\phi x\right)\right]+\frac{\partial}{\partial y}\left[KA_{44}\left(\frac{\partial w_0}{\partial y}+\phi y\right)+KA_{45}\left(\frac{\partial w_0}{\partial x}+\phi x\right)\right] \quad (27)$$
$$+N_{xx}\frac{\partial^2 w_0}{\partial x^2}+2N_{xy}\frac{\partial^2 w_0}{\partial x\,\partial y}+N_{yy}\frac{\partial^2 w_0}{\partial y^2}+q=I_0\frac{\partial^2 w_0}{\partial t^2}$$

(4): $\frac{\partial M_{xx}}{\partial x}+\frac{\partial M_{xy}}{\partial y}-Q_x=I_2\frac{\partial^2 \phi_x}{\partial t^2}+I_1\frac{\partial^2 u_0}{\partial t^2}\Rightarrow$

$$\frac{\partial}{\partial x}\left[B_{11}\frac{\partial u_0}{\partial x}+B_{12}\frac{\partial v_0}{\partial y}+B_{16}\left(\frac{\partial u_0}{\partial y}+\frac{\partial v_0}{\partial x}\right)+D_{11}\frac{\partial \phi_x}{\partial x}+D_{12}\frac{\partial \phi_y}{\partial y}+D_{16}\left(\frac{\partial \phi_x}{\partial y}+\frac{\partial \phi_y}{\partial x}\right)\right]$$
$$+\frac{\partial}{\partial y}\left[B_{16}\frac{\partial u_0}{\partial x}+B_{26}\frac{\partial v_0}{\partial y}+B_{66}\left(\frac{\partial u_0}{\partial y}+\frac{\partial v_0}{\partial x}\right)+D_{16}\frac{\partial \phi_x}{\partial x}+D_{26}\frac{\partial \phi_y}{\partial y}+D_{66}\left(\frac{\partial \phi_x}{\partial y}+\frac{\partial \phi_y}{\partial x}\right)\right] \quad (28)$$
$$-\left[KA_{45}\left(\frac{\partial w_0}{\partial y}+\phi_y\right)+KA_{55}\left(\frac{\partial w_0}{\partial x}+\phi_x\right)\right]-\left(\frac{\partial M^T_{xx}}{\partial x}+\frac{\partial M^T_{xy}}{\partial y}\right)=I_2\frac{\partial^2 \phi_x}{\partial t^2}+I_1\frac{\partial^2 u_0}{\partial t^2}$$

(5): $\frac{\partial M_{xy}}{\partial x}+\frac{\partial M_{yy}}{\partial y}-Q_y=I_2\frac{\partial^2 \phi_y}{\partial t^2}+I_1\frac{\partial^2 v_0}{\partial t^2}\Rightarrow$

$$\frac{\partial}{\partial x}\left[B_{16}\frac{\partial u_0}{\partial x}+B_{26}\frac{\partial v_0}{\partial y}+B_{66}\left(\frac{\partial u_0}{\partial y}+\frac{\partial v_0}{\partial x}\right)+D_{16}\frac{\partial \phi_x}{\partial x}+D_{26}\frac{\partial \phi_y}{\partial y}+D_{66}\left(\frac{\partial \phi_x}{\partial y}+\frac{\partial \phi_y}{\partial x}\right)\right]$$
$$+\frac{\partial}{\partial y}\left[B_{12}\frac{\partial u_0}{\partial x}+B_{22}\frac{\partial v_0}{\partial y}+B_{26}\left(\frac{\partial u_0}{\partial y}+\frac{\partial v_0}{\partial x}\right)+D_{12}\frac{\partial \phi_x}{\partial x}+D_{22}\frac{\partial \phi_y}{\partial y}+D_{26}\left(\frac{\partial \phi_x}{\partial y}+\frac{\partial \phi_y}{\partial x}\right)\right] \quad (29)$$
$$-\left[KA_{44}\left(\frac{\partial w_0}{\partial y}+\phi_y\right)+KA_{45}\left(\frac{\partial w_0}{\partial x}+\phi_x\right)\right]-\left(\frac{\partial M^T_{xy}}{\partial x}+\frac{\partial M^T_{yy}}{\partial y}\right)=I_2\frac{\partial^2 \phi_y}{\partial t^2}+I_1\frac{\partial^2 v_0}{\partial t^2}$$

And:

$$\left(I_0,I_1,I_2\right)=\int_{-h/2}^{h/2}\rho(z)\left(1,z,z^2\right)dz \quad (30)$$

For this problem, I_0,I_1,I_2 are expressed as follows after calculation and integration [17]:

$$I_0=\int_{-H/2}^{H/2}\rho(z)dz=\left(\frac{8}{9}V^*_{CNT}H\left(\rho_{CNT}-\rho_m\right)+\rho_m H\right),$$
$$I_1=\int_{-H/2}^{H/2}\rho(z)z\,dz=0 \quad (31)$$
$$I_2=\int_{-H/2}^{H/2}\rho(z)z^2dz=\left(\frac{H^3}{324}\left(40\,V^*_{CNT}\rho_{CNT}+27\rho_m-40\rho_m V^*_{CNT}\right)\right),$$

And:

$$Q_x = KA_{55}\gamma_{xz}^0, \quad Q_y = KA_{44}\gamma_{yz}^0, \tag{32}$$

Q_x and Q_y are the cross-sectional forces of the plates and K is the shear correction coefficient which is equal to $K=\frac{5}{6}$ [15].

$$(A_{44},A_{55}) = \sum_{k=1}^{N}\left(Q_{44}^k,Q_{55}^k\right)\left(z_{k+1}-z_k\right) \tag{33}$$

SSSS and Navier's solution method are assumed to estimate boundary conditions and equations of motion with FSDT [6].

$$\begin{aligned}
u_0(x,y,t) &= \sum_{m=0}^{M}\sum_{n=0}^{N} U_{mn}\cos(\alpha x)\sin(\beta y)\sin(\omega_{mn}t)\\
v_0(x,y,t) &= \sum_{m=0}^{M}\sum_{n=0}^{N} V_{mn}\sin(\alpha x)\cos(\beta y)\sin(\omega_{mn}t)\\
w_0(x,y,t) &= \sum_{m=0}^{M}\sum_{n=0}^{N} W_{mn}\sin(\alpha x)\sin(\beta y)\sin(\omega_{mn}t)\\
\phi_x(x,y,t) &= \sum_{m=0}^{M}\sum_{n=0}^{N} X_{mn}\cos(\alpha x)\sin(\beta y)\sin(\omega_{mn}t)\\
\phi_y(x,y,t) &= \sum_{m=0}^{M}\sum_{n=0}^{N} Y_{mn}\sin(\alpha x)\cos(\beta y)\sin(\omega_{mn}t)
\end{aligned} \tag{34}$$

Where:

$$\alpha = \frac{m\pi}{b} \text{ and } \beta = \frac{n\pi}{a}$$

By satisfying the boundary conditions by Navier Solution (34) and placing them in equations (25) to (29), the stiffness matrix coefficients for SSSS are calculated:

$$\begin{aligned}
C_{11} &= -(A_{11}\alpha^2 + A_{66}\beta^2)\\
C_{12} &= -\alpha\beta(A_{12}+A_{66})\\
C_{22} &= -(A_{66}\alpha^2 + A_{22}\beta^2)\\
C_{33} &= -K(A_{55}\alpha^2 + A_{44}\beta^2)\\
C_{44} &= (D_{11}\alpha^3 + D_{12}\alpha\beta^2 + 2D_{66}\alpha\beta^2 - KA_{55}\alpha)\\
C_{55} &= (2D_{66}\alpha^2\beta + D_{12}\alpha^2\beta + D_{22}\beta^3 - KA_{44}\beta)
\end{aligned} \tag{35}$$

Other stiffness matrix coefficients are zero according to the condition of the problem:

$$C_{13}=C_{14}=C_{15}=C_{23}=C_{24}=C_{25}=C_{34}=C_{35}=C_{45}=0 \tag{36}$$

6 FREE VIBRATIONS

The following equations are obtained by placing the force and torque equations in terms of displacement from (25) to (29) in motion equations (24):

$$\left([C]-\omega^2[M]\right)\{\Delta\} = \{0\} \tag{37}$$

Here, [C] and [M] are the stiffness matrix and the plate mass matrix, respectively, ω is the natural frequency of the plate and $\{\Delta\}$ is the displacement vector. Mass matrix coefficients and the stiffness of the plate are as follows:

$$[C] = \begin{bmatrix} C_{11} & C_{12} & 0 & 0 & 0\\ C_{12} & C_{22} & 0 & 0 & 0\\ 0 & 0 & C_{33} & 0 & 0\\ 0 & 0 & 0 & C_{44} & 0\\ 0 & 0 & 0 & 0 & C_{55} \end{bmatrix} \tag{38}$$

And:

$$[M] = \begin{bmatrix} M_{11} & 0 & 0 & 0 & 0\\ 0 & M_{22} & 0 & 0 & 0\\ 0 & 0 & M_{33} & 0 & 0\\ 0 & 0 & 0 & M_{44} & 0\\ 0 & 0 & 0 & 0 & M_{55} \end{bmatrix} \tag{39}$$

Where:

$$\begin{aligned}
&M_{ij} = M_{ji}\\
&M_{11} = M_{22} = M_{33} = I_0\\
&M_{44} = M_{55} = I_2\\
&\text{all other } M_{ij} = 0
\end{aligned} \tag{40}$$

Thus:

$$\left\{\begin{bmatrix} C_{11} & C_{12} & 0 & 0 & 0 \\ C_{12} & C_{22} & 0 & 0 & 0 \\ 0 & 0 & C_{33} & 0 & 0 \\ 0 & 0 & 0 & C_{44} & 0 \\ 0 & 0 & 0 & 0 & C_{55} \end{bmatrix} - \omega^2 \begin{bmatrix} M_{11} & 0 & 0 & 0 & 0 \\ 0 & M_{22} & 0 & 0 & 0 \\ 0 & 0 & M_{33} & 0 & 0 \\ 0 & 0 & 0 & M_{44} & 0 \\ 0 & 0 & 0 & 0 & M_{55} \end{bmatrix}\right\} \begin{Bmatrix} U_{mn}^{0} \\ V_{mn}^{0} \\ W_{mn}^{0} \\ X_{mn}^{0} \\ Y_{mn}^{0} \end{Bmatrix} = 0 \quad (41)$$

Moreover, the natural frequencies of the problem are obtained with different conditions. Besides, the natural frequency without a dimension is obtained from Equation (42) [13]:

$$\bar{\omega}_{mn} = \omega_{mn} \frac{a^2}{h} \sqrt{\frac{\rho_m}{E_m}} \quad (42)$$

7 FINITE ELEMENT ANALYSIS

Vibrational analysis of the plate is done in ABAQUS 6.14.1. The dimensions of the nanocomposite plate model include a length of 40 cm, a width of 20 cm and a thickness of 33 mm.

8 MECHANICAL PROPERTIES OF CARBON NANOTUBE REINFORCED PLATES

The problem model consists of a three-layer structure where layers (1) and (3) are similar in terms of dimensions and distribution of nanotubes and so have the same properties. Layer (2) only has the isotropic matrix. The type of CNTs used in this study is SWCNT (10, 10), according to "Tables 1 and 2".

9 RESULTS AND DISCUSSION

As "Fig. 2a" shows, the natural frequency without a dimension is higher in the third mode than in the first and third modes according to the diagram data, and FEM has a higher natural frequency without dimension in the third mode. Figure 2b shows that the natural frequency in all three methods in mode (1 and 1) is the highest because it is thicker than the previous figure. The highest frequencies are FEM, FSDT and Matrix, respectively. Moreover, it has a higher frequency in the third FEM mode. In "Fig. 2c", the natural frequency changes in the first to third modes are minimal for each method;

Table 1 Mechanical properties of CNT and matrix [18]

G_m	υ_m	E_m	ρ_m	G_{12}^{CNT}	E_{22}^{CNT}	E_{11}^{CNT}	υ_{12}^{CNT}	ρ^{CNT}
0.7835 GPa	0.34	2.1 GPa	1500 kg/m^3	1.9445 TPa	7.08 TPa	5.6466 TPa	0.175	1400 kg/m3

Table 2 Mechanical properties of CNTRC plates relative to the percentage of carbon nanotubes

η_3	η_2	η_1	ρ	υ_{12}	G_{12} GPa	E_{22} GPa	E_{11} GPa	% NTC
0.653	0.934	0.149	1489	0.3218	0.851	3.258	92.54	**0.11**
0.658	0.941	0.150	1486	0.3169	0.88	3.372	117.78	**0.14**
0.966	1.381	0.149	1483	0.3119	0.9125	3.49388	143	**0.17**

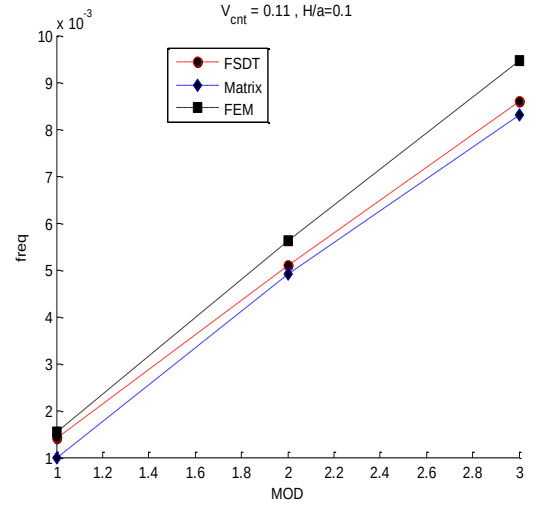

a

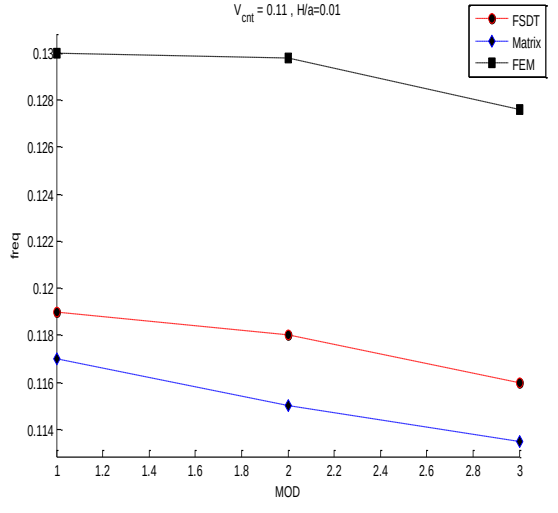

b

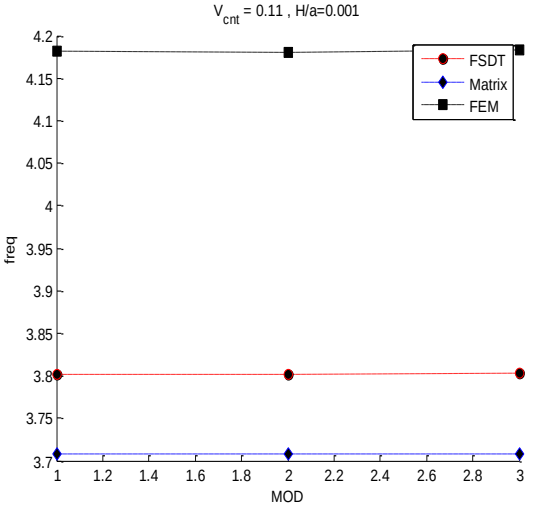

c

Fig. 2 Frequency changes of first to third modes relative to different H / a and VCNT = 0.11.

Thus, according to the diagram, the highest frequencies are related to FEM, FSDT and Matrix, respectively.

Figure 3a is almost identical to "Fig. 2a" in terms of shape and function. The difference is that the volume fraction in this graph is equal to VCNT = 0.14. Figure 3b is stated as the calculated frequencies of the first mode in the two methods of solving FSDT and Matrix are somehow the same. In contrast, unlike the previous figures, the numerical solution of FEM has lesser value, and in the third mode, FSDT has a higher frequency than Matrix.

In Figure 3c, there are interesting points to present. According to the figure, it is seen that the frequency changes in the first to third modes of Matrix are such that in the third mode the frequency is higher than the first mode. However, the frequency changes in FSDT and FEM are partial, but in the first mode the frequency is higher than the second and third modes.

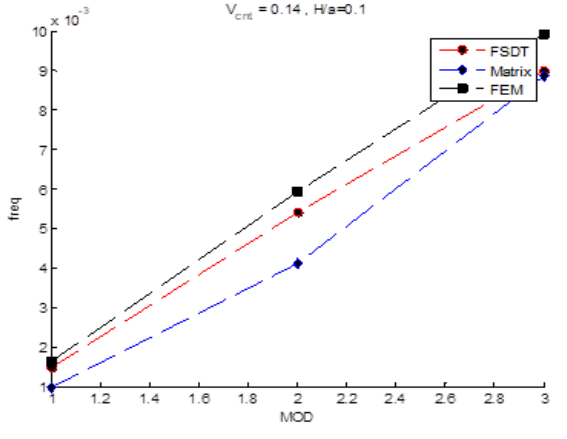

a

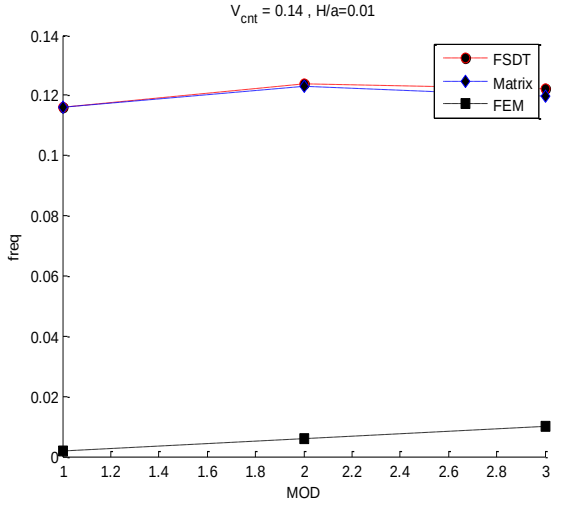

b

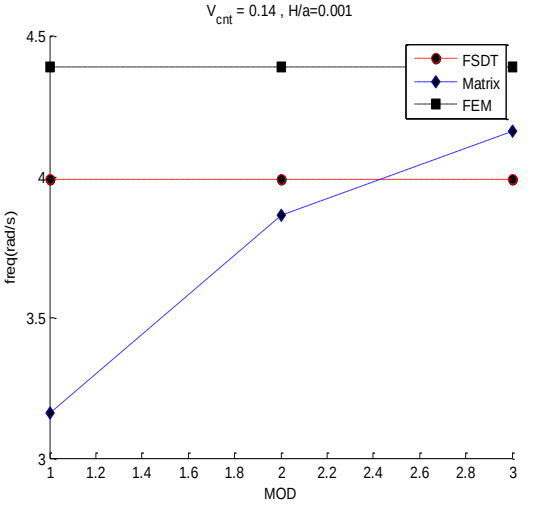

C

Fig. 3 Frequency changes of the first to third modes relative to H / a = 0. 1, 0. 01, 0. 001 and VCNT = 0.14.

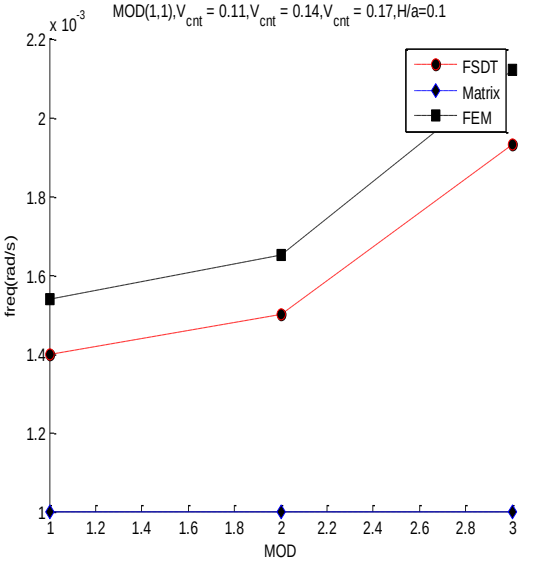

Fig. 4 Mode changes (1 and 1) relative to the increase in the volume fraction with coefficient H / a = 0.1

Figures 4 to 6 show the changes of dimensionless natural frequencies in the first mode with a constant H / a, relative to the volume fraction, showing that the frequency changes in the first mode are constant and equal for the polymer because no changes have occurred in its material.

However, in other methods (FEM, FSDT), as the volume fraction of carbon nanotubes changes, the natural dimensionless frequencies are different from each other, and the largest natural dimensionless frequency is related to the volume fraction VCNT = 0.17, which is different according to the analytical method.

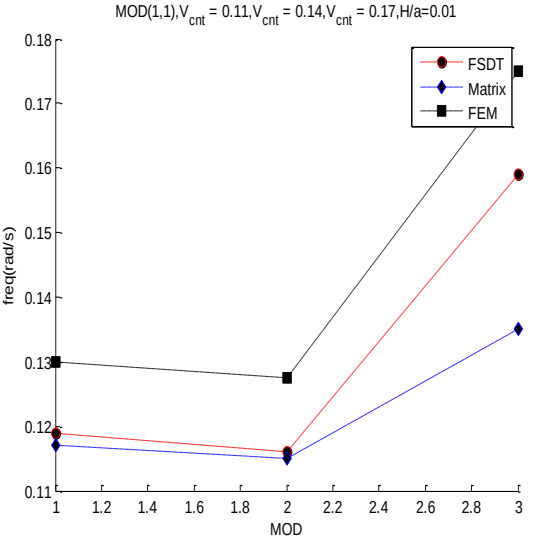

Fig. 5 Mode changes (1 and 1) relative to H / a = 0.01 and different VCNT.

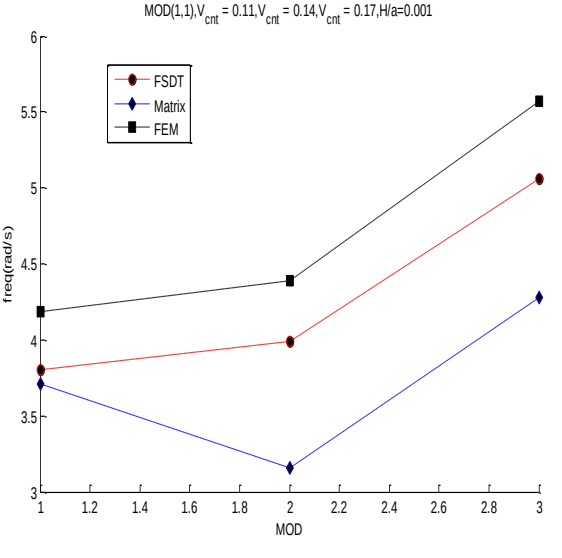

Fig. 6 Mode changes (1 and 1) relative to the increase in the volume fraction with coefficient H / a = 0.001.

10 THE RESULTS OF FINITE ELEMENT ANALYSIS

In "Figs.7, 8 and 9", the shape of the vibrational mode of the desired plate is presented in different frequencies.

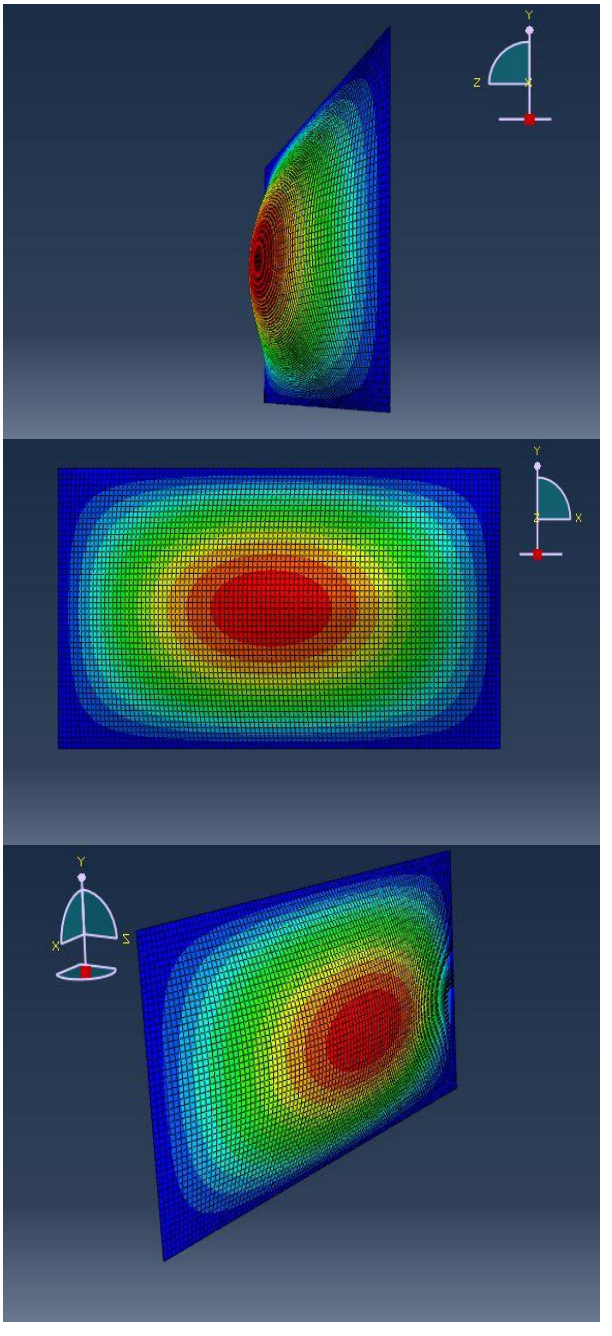

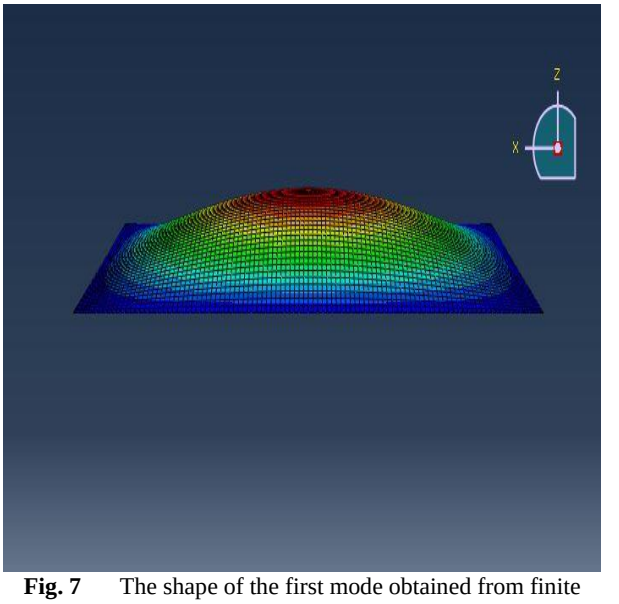

Fig. 7 The shape of the first mode obtained from finite element analysis, mode (1 and 1).

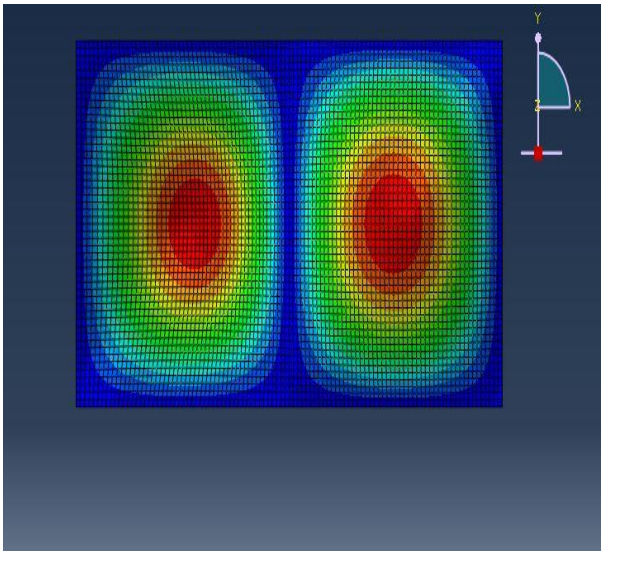

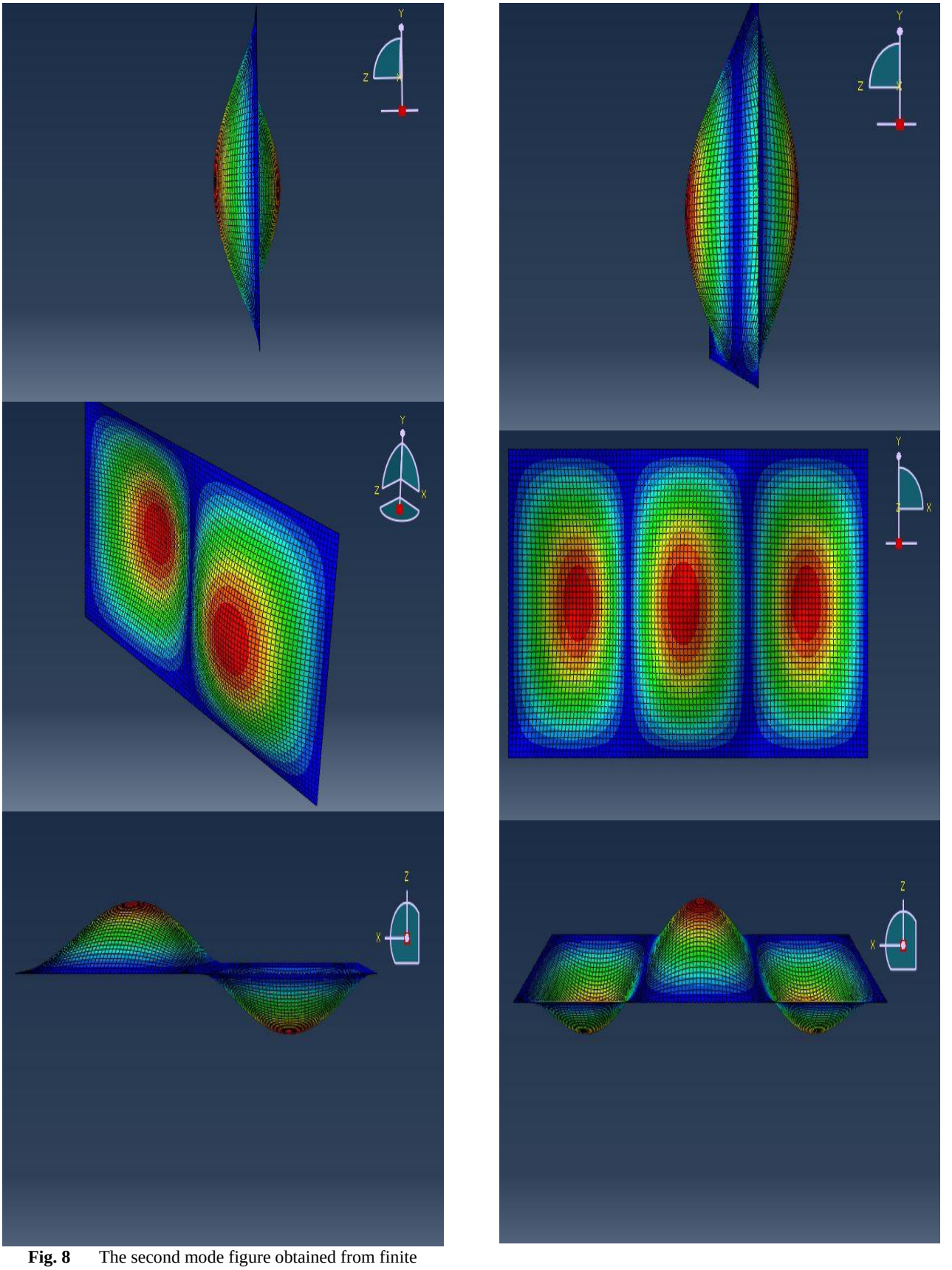

Fig. 8 The second mode figure obtained from finite element analysis, mode (1 and 2).

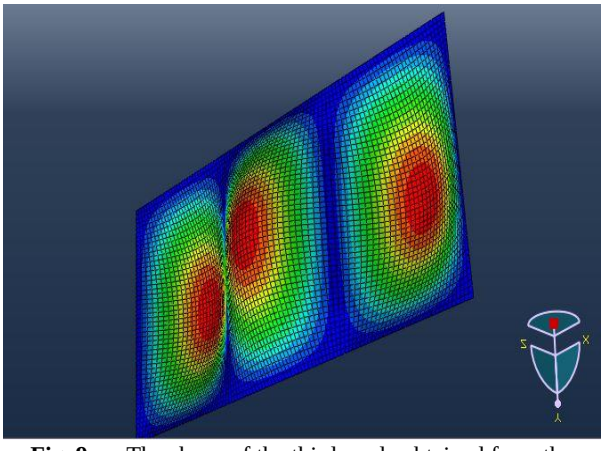

Fig. 9 The shape of the third mode obtained from the finite element solution, modes (1 and 3).

11 CONCLUSION

The purpose of this project is to examine the effect of adding carbon nanotubes to the polymer on the dynamic properties of the structure (natural frequencies). In this study, the effect of volume fraction of nanotubes, thickness to length ratio, geometric shape and their purposeful distribution in improving the vibrational properties of the structure using the analytical method and finite element were examined. The boundary conditions (SSSS) using Fourier series were considered for this. The results obtained from the analytical solution by FSDT method and the results from finite element software are presented, the results of which are summarized as follows:

A) Dimensionless natural frequencies increase as carbon nanotubes increase.

B) Dimensionless natural frequencies decrease as the page thickness-to-length ratio increases.

C) Carbon nanotubes are a great candidate for low-weight, high-strength composite structures given their excellent mechanical properties. The most significant reason that can be stated is that it has a lower density and specific volume than a polymer.

D) The shape of the modes obtained from finite element analysis and the results of the analytical solution are in line with each other.

E) Since adding carbon nanotubes has little effect on increasing the modulus of the polymer, the increase in natural frequencies will not be so high. The maximum frequency increase for SWNT sample is 17% in the first mode with a ratio about Rad/s.

F) The highest frequency value in all vibrational modes is seen for SWCNT 17%, SWCNT 14% and SWCNT11%, respectively. Hence, one can conclude that the best mechanical properties are obtained by adding, respectively, 17%, 14% and 11% by weight of SWCNT to the composite.

G) According to the results, one can conclude that the nanocomposite plate with H / a = 0.001 and VCNT = 0.17 is a good candidate for the model.

H) The examinations performed in the study show that the ratio of plate thickness-to-length has an effective role in enhancing the frequencies of the first mode. Here, in all three-volume fractions, nanotubes showed better vibrational modes compared to the previous two modes.

I) In case that there is a polymer layer without nanotubes in the laminate, the natural frequency in the structure will reduce.

REFERENCES

[1] Iijima, S., Helical Microtubules of Graphitic Carbon, Nature, Vol. 354, 1991, pp. 56–58.

[2] Asadi, E., Manufacturing and Experimental Study of Vibration of Laminated Composite Plates Reinforced by Carbon Nano-Tube, MSc Thesis, Malek-Ashtar Uuniversity of Technology, Iran, 2013.

[3] Lei, Z. X., Liew, K. M., and Yu, J. L., Free Vibration Analysis of Functionally Graded Carbon Nanotube-Reinforced Composite Plates Using the Element-Free kp-Ritz Method in Thermal Environment, Compos. Struct., Vol 106, 2013, pp. 128-138.

[4] Rahim. Nami, M., Janghorban, M., Free Vibration of Thick Functionally Graded Carbon Nanotube-Reinforced Rectangular Composite Plates Based On Three-Dimensional Elasticity Theory via Differential Quadrature Method, Advanced composite Materials, 2014, pp. 439-450.

[5] Akbar. Alibeigloo, Ali. Emtehani, Static and Free Vibration Analyses of Carbon Nanotube-Reinforced Composite Plate Using Differential Quadrature Method, Meccanica, Vol. 50, 2015, pp. 61-76.

[6] Amraei, J. Emami, J., and Jam, J. E., Free Vibrations of Laminated Rectangular Plate Reinforced With Carbon Nanotubes, Wiley, DOI 10.1002/pc.23788, Polymer Composites-2015.

[7] Dinh Dat, N., Quoc Quan, T., Mahesh, V., and Dinh Duc, N., Analytical Solutions for Nonlinear Magneto-Electro-Elastic Vibration of Smart Sandwich Plate with Carbon Nanotube Reinforced Nanocomposite Core in Hygrothermal Environment, International Journal of Mechanical Sciences, Vol. 186, 2020, 105906,

[8] Formica, G., Lacarbonara, W., and Alessi, R., Vibrations of Carbon Nanotube-Reinforced Composites, Journal of Sound and Vibration, Vol. 329, No. 10, 2010, pp. 1875-1889.

[9] Esawi, A. M. K., Farag, M. M., Carbon Nanotube Reinforced Composites: Potential and Current Challenges, Mater Des, Vol. 28, 2007, PP. 2394–401.

[10] Fidelus, J. D., Wiesel, E., Gojny, F. H., Schulte, K., and Wagner, H. D., Thermo-Mechanical Properties of Randomly Oriented Carbon/Epoxy Nanocomposites, Compos Part A: Appl Sci Manuf, Vol. 36, 2005, pp.

1555–61.

[11] Shen, S., Nonlinear Bending of Functionally Graded Carbon Nanotube Reinforced Composite Plates in Thermal Environments, Compos Struct, Vol. 91, 2009, pp. 9–19.

[12] Zhu, P., Lei, Z. X., and Liew, K. M., Static and Free Vibration Analyses of Carbon Nanotube Reinforced Composite Plates Using Finite Element Method with First Order Shear Deformation Plate Theory, Compos Struct, Vol. 94, 2012, pp. 1450–60.

[13] Lei, Z. X., Liew, K. M., and Yu, J. L., Free Vibration Analysis of Functionally Graded Carbon Nanotube-Reinforced Composite Plates Using the Element-Free Kp-Ritz Method in Thermal Environment, Compos. Struct., Vol. 106, 2013, pp. 128-138.

[14] Phuc Phung, V., Magd Abdel, W., Liew, K. M., Bordas, S. P. A., and Nguyen-Xuan, H., Isogeometric Analysis of Functionally Graded Carbon Nanotube-Reinforced Composite Plates Using Higher-Order Shear Deformation Theory, Composite structures, vOL. 123, 2015, pp. 137-149.

[15] Reddy, J. N., Mechanics of Laminated Composite Plates and Shells: Theory and Analysis, CRC Press LLC, The United States of America, 2004.

[16] Zhang, L. W., Lei, Z. X., and Liew, K. M., Vibration Characteristic of Moderately Thick Functionally Graded Carbon Nanotube Reinforced Composite Skew Plates, Composite Structures, Vol. 122, 2015, pp. 172-183.

[17] Moradi.Dastjerdi, R., Stress Distribution in Functionally Graded Nanocomposite Cylinders Reinforced by Wavy Carbon Nanotube, Advanced Design and Manufacturing Technology, Vol. 7, No. 4, 2014, pp. 43-54.

[18] beigloo, A., Emtehani, A., Static and Free Vibration Analyses of Carbon Nanotube-Reinforced Composite Plate Using Differential Quadrature Method, Meccanica, 2015, 50. 10.1007/s11012-014-0050-7.